Int. J. Multiphase Flow Vol. 19, No. 4, pp. 691–704, 1993
Printed in Great Britain.

0301-9322/93 $6.00 + 0.00

PERCOLATION MODEL OF DRYING UNDER ISOTHERMAL CONDITIONS IN POROUS MEDIA

M. PRAT
Institut de Mécanique des Fluides de Toulouse, avenue du Professeur Camille Soula, 31400 Toulouse, France

(Received 30 September 1992; in revised form 14 April 1993)

Abstract—A model of drying of capillary porous media is presented based on a modified form of invasion percolation theory. The porous medium is conceptualized as a network of pores connected by narrow throats. In addition to capillary and gravity effects, evaporation at the microscopic gas–liquid interface and vapor diffusion in the gaseous phase are taken into account. This leads to a modification of the invasion rules associated with invasion percolation. The simulations on a two-dimensional network containing 5000 ducts compare favorably with experimental results obtained by means of a two-dimensional micromodel.

Key Words: porous media, drying, invasion percolation, microscopic simulator

1. INTRODUCTION

Evaporation processes in porous media are observed in many fields spanning from drying of various materials to vaporization processes of liquid hydrocarbons in connection with secondary oil recovery techniques in petroleum engineering. However, even the simplest situation, such as the convective drying of a bed of glass beads at room temperature, is still a challenging problem for the modelers. Traditionally, the problem is treated within the framework of the continuum approach to porous media (Whitaker 1977). This approach, which relies on the generalized Darcy's law and the relative permeability concept, amounts to modeling the porous medium, which is an heterogeneous multiphase system, as a system of fictitious continuum media. As discussed by Masmoudi *et al.* (1992), the relevance of this traditional approach has not yet been fully demonstrated. In fact, the shortcomings of the continuum approach, such as, for instance, the lack of a general method for predicting interfacial mass transfer coefficients for convective drying, lead one to reconsider the problem entirely and to develop a completely different approach (Plumb & Prat 1992). In the present study, a model describing the relevant phenomena at the pore level, as opposed to the continuum level in the case of the traditional approach, during the drying process is presented. Making use of this model, together with appropriate averaging operators, should eventually lead to an assessment of the relevance of the traditional continuum model. This objective, however, is beyond the scope of this paper, which is essentially devoted to a presentation of the pore level or "microscopic" model.

In order to consider the simplest situation presenting the essential features of drying of capillary porous media, we consider the isothermal drying of a capillary porous medium initially fully saturated by liquid. The terminology "capillary porous medium" implies that capillary effects are the main mechanism of internal moisture transfer in the liquid phase and that, therefore, contrary to hygroscopic materials, water sorption phenomena may be neglected. In such a drying process, evaporation causes a liquid–air interface to form and to move within the porous medium. At the very beginning of the process, evaporation causes the liquid–air interface to recede into the pore channels at the surface of the medium. At the threshold capillary pressure value associated with the largest pore channel at the surface (according to Laplace's law, capillary pressure is a decreasing function of the pore diameter), the largest pore channel at the interface is invaded and the meniscus advances to the next constriction. The liquid that was contained in the pore is transported to the evaporating surface through the saturated pores. Then, a similar process takes place and a subsequent pore is invaded. Thus, air progressively invades the porous structure displacing the liquid towards the evaporating surface through remaining saturated regions. Here,

the evaporating surface should be understood as a surface made up of each elementary gas–liquid interface at which evaporation takes place. As we shall see, the shape of this surface is quite complicated. Therefore, drying can be, to a certain extent, viewed as an immiscible displacement process in which the gaseous phase is the invading phase (Shaw 1987). Even though, as we shall see in the following, drying possesses some very specific characteristics, our drying model partly relies on concepts developed for analyzing conventional two-fluid immiscible displacements. For instance, in the present approach, the porous medium is conceptualized as a network of pores joined by narrow connecting throats which is similar to those used in many fluid displacement studies, see Lenormand *et al.* (1988) among many others. Furthermore, Lenormand *et al.* (1988) have shown that, in the absence of gravity, conventional immiscible displacements can be characterized by two dimensionless numbers: the viscosity ratio M and the capillary number Ca:

$$M = \frac{\mu_{df}}{\mu}, \qquad \mathrm{Ca} = \frac{\mu v}{\sigma},$$

where μ_{df} is the displacing fluid viscosity, μ is the displaced fluid viscosity, σ is the interfacial tension and v is the displaced fluid average or "macoscopic" velocity. In the case of drying, Ca is generally very small, typical values are smaller than $< 10^{-10}$. As Ca measures the ratio of the viscous forces to the capillary forces, it can be concluded that here capillary forces are the dominant ones as far as the liquid transport is concerned. According to Lenormand *et al.* (1988), at comparable Ca immiscible displacements produce capillary fingering. Such displacements at very low Ca can be associated with invasion percolation as a statistical model (Chandler *et al.* 1982; Wilkinson & Willemsen 1983; Lenormand *et al.* 1988). In its standard formulation, Wilkinson (1986) and references therein, invasion percolation describes the capillary displacements of two immiscible fluids. Our model differs from the standard two-fluid displacement model at low Ca because of the combined actions of evaporation, vapor diffusion in the gaseous phase and capillary mechanisms. Essentially, this requires one to solve the diffusion problem in the gaseous phase at each elementary step of the process and leads us to modify the invasion rules associated with invasion percolation. It should be also emphasized that, in general, gravity effects cannot be neglected because of the great difference in density between the liquid phase and the gaseous phase. Taking into account gravity forces is accomplished according to the method suggested by Wilkinson (1984).

Making use of percolation concepts for analyzing moisture migration in unsaturated porous media is not a novelty. For instance, Quenard (1989) relies on some elements of percolation theory in his study about water-vapor adsorption and transfer in microporous media. In the same spirit, Daian & Saliba (1991) have studied the moisture migration in cement mortar. However, our work differs completely from these studies in which a network is used to model a representative elementary volume (REV) of the porous structure, see for instance Bachmat & Bear (1986), as opposed to the whole structure in our approach. More specifically, we do not *a priori* postulate the appropriateness of the concept of the REV for the process under investigation. As a matter of fact, one future use of the present model will be to explore the relevance of the REV concept in the case of drying. Also, the invasion rules developed in the present study have little to do with those used by Quenard (1989) and Daian & Saliba (1991), who were essentially interested mainly in determining macroscopic transport and equilibrium properties of hygroscopic materials as opposed to our approach which describes a dynamic invasion process in capillary porous media.

The paper is organized as follows. In section 2, the two-dimensional network used in the numerical simulation is presented. The drying model is described in section 3. It is worth clarifying that the drying model itself is not limited to two-dimensional networks. Three-dimensional networks could be perfectly considered. Results of the simulation and comparisons with experiments are presented in section 4. Conclusions and future research directions are discussed in section 5.

2. NETWORK MODEL

The porous medium is represented by a two-dimensional network of randomly sized pores joined by randomly sized throats which is similar to that used by Lenormand *et al.* (1988). The pores and the throats are located, respectively, at the sites and bonds of a two-dimensional square lattice,

figure 1. The width of each throat is randomly chosen according to a given distribution law (we used here a log normal distribution). A network is fully characterized by three parameters: the distribution law; the distance a between two nodes; and the space distribution coefficient β between the pore and throat [$a = \beta a + (1 - \beta)a$, in which βa represents the typical length of a throat], figure 2. In this description, the porosity of the network can be selected by choosing an appropriate value of β in the interval (0, 1). The simulations presented in section 4 have been performed on a 50×50 network containing about 5000 throats. This network, the porosity of which is 0.4, has been chosen because it presents the same basic characteristics as the micromodel used in the experiments, see section 4.

Initially, the network is fully saturated with a liquid which is assumed to be the wetting fluid. Evaporation takes place by allowing the liquid to evaporate from the open edge of the network which is the top edge in figure 1. No transfer is allowed through the three remaining edges of the network.

3. DRYING MODEL

As our model relies on a modified form of invasion percolation, it is useful to first consider briefly the standard form of invasion percolation (Wilkinson 1986).

3.1. Standard invasion percolation

Invasion percolation has been developed in order to describe two-fluid immiscible displacements at very low Ca in relation to secondary oil recovery. For simplicity, let us consider the process of a wetting fluid being displaced from a network similar to the one described in section 2. In the limit of very small flow rates, viscous forces can be neglected and the displacement process is completely dominated by the capillary forces acting at the wetting fluid non-wetting fluid interfaces. Note that gravity forces are neglected. The invasion process is analyzed as follows. At each step in the displacement process, the non-wetting fluid can only enter the throat associated

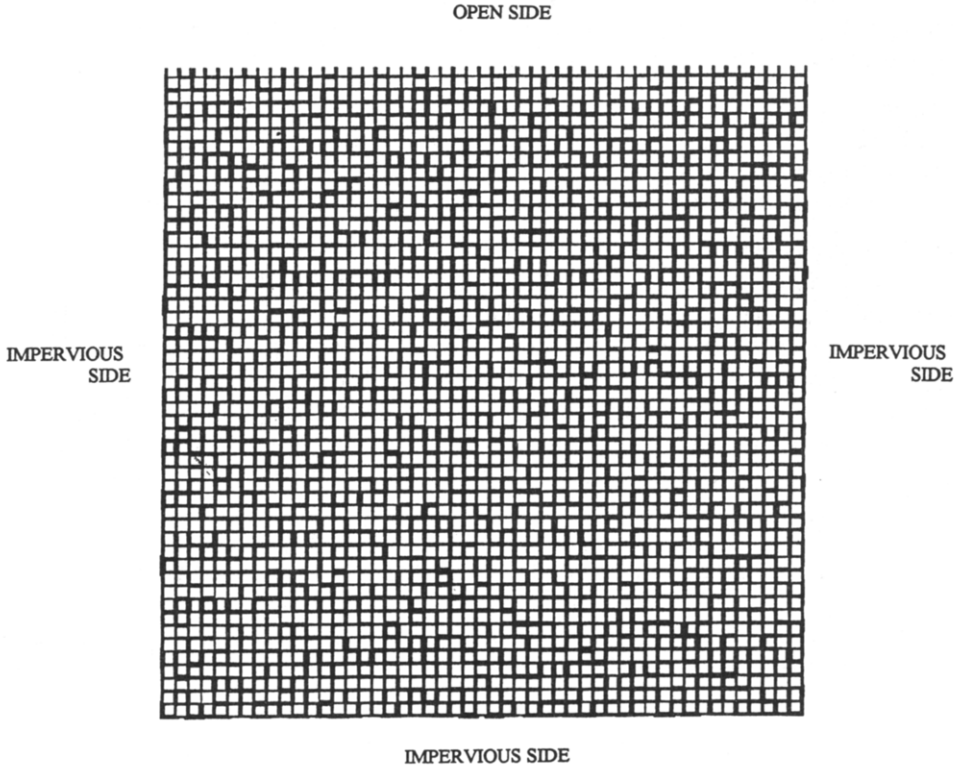

Figure 1. Two-dimensional 50×50 network.

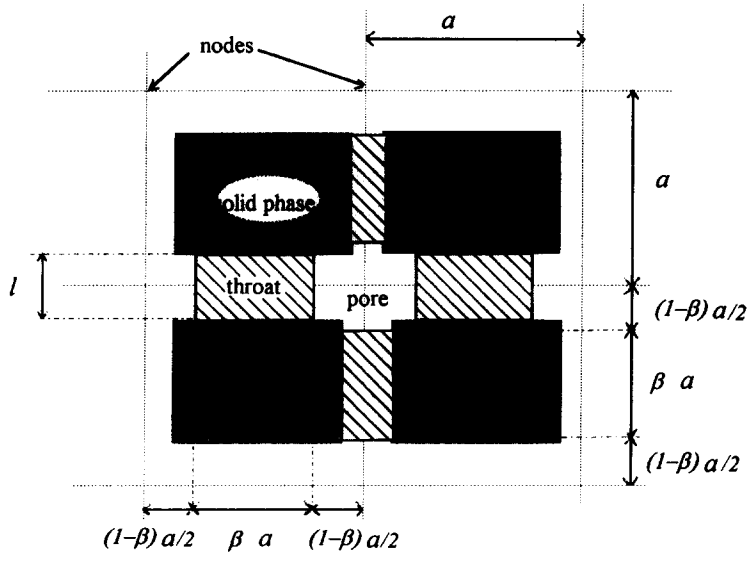

Figure 2. Definitions and geometrical parameters of the network.

with the smallest capillary pressure, i.e. the throat having the greatest width. Thus, at each step, the displacing fluid invades one throat together with the adjacent pore according to the width of the throats along the frontier between the two fluids within the network. This process results in the occurrence of trapped regions of the wetting fluid, i.e. regions of the wetting fluid completely surrounded by the non-wetting fluid. Because of the trapping phenomenon, an additional rule should be satisfied. A throat located in a trapped region cannot be invaded because of the fluid incompressibility. In other words, a throat can be invaded only if the throat is connected to some outlet face. As emphasized by Wilkinson (1986), the trapping rule is what makes invasion percolation different from usual percolation, see for instance Stauffer (1985).

Therefore, in the case of a drainage process and for a network similar to the one considered in the present study, the invasion percolation rules can be summarized as:

(1) At each step, the displacing fluid invades the widest accessible throat.
(2) Regions of the wetting fluid which become disconnected from the outlet face cannot be invaded and are trapped.
(3) The process ends when none of the wetting fluid is connected to the outlet face.

For the 50 × 50 network shown in figure 1, making use of the invasion percolation rules leads to the phase distribution within the network depicted in figure 3 at the completion of the drainage. Here, it was assumed that the displacing fluid can enter at the top edge of the network and that the displaced fluid can also escape through the top edge, no-flow conditions being imposed at the other edges. It is worth noting that such a drainage process would be very difficult to perform experimentally. However, for the sake of comparison with the drying process it is clearly of interest to consider this particular case rather than more traditional configurations. As can be seen from figure 3, drainage results in permanently trapped wetting fluid clusters of various sizes.

3.2. Invasion percolation model of drying in the absence of gravity forces

Standard invasion percolation accounts for capillary effects. In the absence of gravity forces, drying is not only controlled by capillary effects but also by the evaporation taking place at the non-wetting fluid–wetting fluid, i.e. gas–liquid, interfaces and the vapor diffusion within the gaseous phase. Therefore, the invasion rules should be modified to account for drying-specific features. The new rules are based on the following observations:

- Because of capillary effects similar to those observed in standard immiscible displacement at low Ca, regions of the wetting fluid can be completely surrounded by the non-wetting fluids. This results in the occurrence of disconnected wetting

fluid regions of various size within the network. Such a region is called hereafter a temporary wetting fluid cluster (TC).

- Because evaporation takes place at each elementary non-wetting fluid–wetting fluid interface, the trapping rule of standard invasion percolation is no longer valid. In other words, a throat located in a TC can be invaded as well as a throat located in the main wetting fluid region (which in fact is also a TC).
- Whether or not a throat and its adjacent pore is invaded at a given step of the process depends on its width through the smallest capillary pressure constraint and on the evaporation flux at the frontier of the TC in which the throat is located.

Clearly, at each step of the invasion process, each TC must be identified and the evaporation flux at the frontier of each identified TC must be determined. Furthermore, contrary to standard invasion percolation, permanent trapping of wetting fluid does not occur. The temporary clusters are progressively eliminated under the action of evaporation.

Consequently, the selection of the throat to be invaded at each step of the drying process is based on the following procedure:

(1) Each TC is identified.
(2) The evaporation flux at the boundary of each identified TC is determined by computing the vapor partial pressure field within the gaseous phase.
(3) For each TC, the throat of greatest width located at the frontier of the TC is identified.
(4) For each TC, the mass loss associated with the evaporation flux determined in step (2) is assigned to the throat identified in step (3).
(5) The throat eventually selected is that which is the first to be completely drained among the throats selected in step (3).
(6) The phase distribution within the network is updated and the above-described procedure is repeated.

Step (2) is accomplished by solving the diffusion equation in the vapor phase, see the appendix. In the present version of the model, the diffusion problem is simplified by solving the

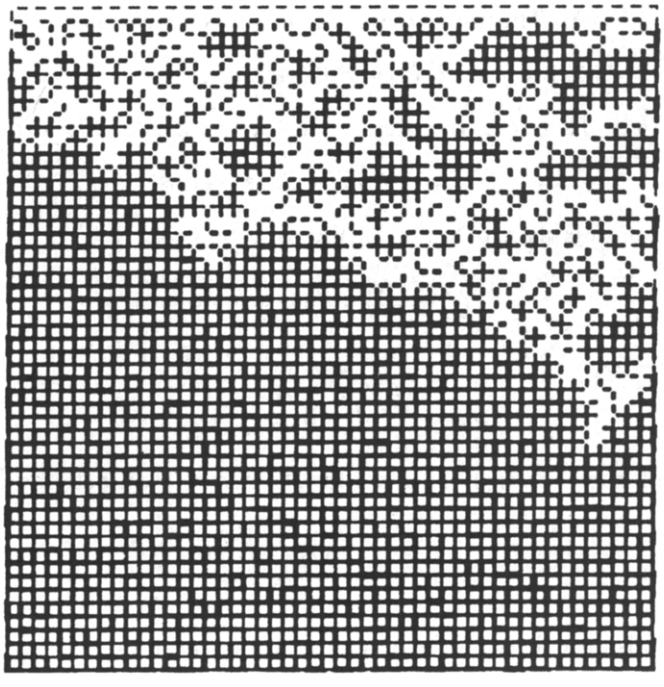

Figure 3. Phase distribution at the completion of the drainage. Pores and throats occupied by the wetting fluid are shown in black. The non-wetting fluid has entered and the wetting fluid has escaped at the top.

one-dimensional steady-state diffusion problem in each throat. Furthermore, we assume that the pores and throats are large enough so that the Kelvin effect, i.e. the influence of the curvature of the liquid–gas interfaces on the equilibrium vapor pressure at the interfaces, may be neglected. Therefore, at the gas–liquid interfaces, the partial vapor pressure is assumed to be the saturation vapor pressure at a flat interface. The end result is a resistance network which is solved numerically to determine the vapor flux at the boundary of each TC. Clearly, a boundary condition should be imposed at the open edge of the network in order to supply the driving potential for the drying process. This external boundary condition, however, does not influence the invasion process topology (i.e. the evolution of the phase distribution within the network) in the limit of small Ca. The dynamics of the process depends on this boundary condition. In this paper, we focus on the events within the network in terms of phase distribution. The analysis of the external boundary condition will be the subject of a future study.

In terms of the liquid flow, it is worth noting that viscous effects are completely ignored. In the limit of very small Ca, hydrostatic equilibrium is assumed at each step of the invasion process.

3.3. Invasion percolation model of drying in the presence of gravity forces

Since we deal with a two-phase transport process involving a liquid and a gaseous phase, gravity forces cannot generally be neglected since the liquid density is much greater than the gas density under usual circumstances. To take into account the gravity forces, we follow the method presented by Wilkinson (1984) for studying immiscible displacements at low Ca in the presence of buoyancy forces. Essentially, this amounts to modifying step (3) of the invasion procedure described in section 2.2. When the gravity forces are neglected, section 2.2, step (3) consists of identifying the throat of greatest width in each TC. In fact, this can be expressed in terms of potential. The potential of a throat can be defined as

$$Q = f(l), \qquad [1]$$

where f is a monotonically increasing function and l is the width of the throat. Consequently, step (3) consists of identifying the throat of each TC having the greatest potential (note that the greatest potential corresponds to the lowest capillary pressure). Under these circumstances, taking into account the gravity forces amounts to making the potential associated with each throat depend on gravity. Assuming that at any instant the system is in vertical equilibrium, the gravity forces balance the capillary forces. Therefore, the capillary pressure depends linearly on the height z:

$$P_c(z) = P_c(0) + \Delta\rho g z, \qquad [2]$$

where $\Delta\rho = \rho_{\text{liquid}} - \rho_{\text{gas}}$. Therefore, the pressure in the liquid is of the form

$$P_l(z) = -P_c(0) - \Delta\rho g z + \text{const.} \qquad [3]$$

Thus, this leads to considering a potential of the form

$$Q_g = -\frac{\sigma}{l} + \Delta\rho g z + \text{const}, \qquad [4]$$

which can be written as

$$Q_g = -\frac{\sigma}{l}\left(1 - \mathrm{B}\frac{lz}{a^2}\right) + \text{const}, \qquad [5]$$

where B is the Bond number which accounts for the competition between capillary and gravity forces:

$$\mathrm{B} = \frac{\Delta\rho g a^2}{\sigma}, \qquad [6]$$

in which a is the distance between two nodes of the network, see section 2. Under these circumstances, the procedure for computing the invasion process is identical to that described in section 2.2 except that step (3) is performed by using [5] instead of a potential of the form given by [1].

4. SIMULATIONS

In this section, the results of the numerical simulations are compared with:

—experimental results obtained by means of a two-dimensional transparent micromodel

and

—simulations performed by making use of the standard invasion percolation rules, section 3.1, without the trapping rule.

4.1. Experiment with a two-dimensional micromodel

This micromodel is a transparent etched network similar to those used by Lenormand *et al.* (1988) in their immiscible displacement study. The micromodel used here contains about 5000 ducts with seven classes of width selected from the interval [0.1 mm, 0.6 mm] according to a distribution law similar to that used for the numerical network. The micromodel is initially fully saturated with alcohol. Drying takes place at room temperature by allowing the alcohol to evaporate from the remaining open edge of the micromodel. Several drying experiments have been carried out for various B values. These have been obtained by modifying the inclination angle α of the micromodel with respect to the horizontal. When the micromodel is held horizontal, $\alpha = 0$ and the gravitational effects are negligible. When the micromodel is held vertical, $\alpha = 90^\circ$ and B is a maximum. Intermediate values of B are obtained for intermediate values of α. Photographs, allowing a direct observation of the phase distribution within the micromodel, were taken at different times during the drying process [for more details concerning the experimental procedure the reader is referred to Masmoudi (1990)].

Figure 4 shows the phase distribution within the micromodel at three different steps of drying in the absence of gravity forces. As can be seen from figure 4, the phase distributions obtained numerically compare favorably with the experimental ones. When the gravity forces are not negligible, the phase distributions depicted in figure 5 were obtained. In figure 5, these phase distributions are compared to those obtained numerically for various B values. Here, it should be emphasized that it has not yet been possible to use exactly the same network for carrying out the numerical simulations and for building the micromodel. Although the two networks, the experimental one and the numerical one, are statistically equivalent, their relatively small sizes prevent a perfect agreement. A more convincing comparison will be made in the future by using the same basic structure for the experiments and the simulations. However, the present qualitative comparison is very encouraging. It can be concluded that the present model captures the essential features of the drying process.

In terms of phase distribution, three main zones can be distinguished:

—Saturated regions.
—Dry regions where transport occurs in the gaseous phase.
—Temporary disconnected liquid cluster regions where water transport is the result of a complex interaction between liquid transport within the clusters and vapor diffusion in the surrounding gaseous phase.

Concerning the temporary cluster region, a careful examination of the photographs seems to indicate that the clusters are not disconnected. In fact, the solid phase is coated with a very thin liquid film in this region. However, the role played by the film in the transport process is still unclear. In the author's opinion, however, most of the transport process can be analyzed in terms of the combined action of liquid transport within the clusters and vapor diffusion in the gaseous phase without taking into account the films. In the absence of gravity forces, these three main regions are quite difficult to distinguish, as can be seen from figure 4. The action of gravity results in the occurrence of a well-defined temporary cluster region which takes place between the saturated region and the dry region, see figure 5. The width of this transition region tends to decrease as B increases. The number and size of the clusters also decrease as B increases.

One interesting feature of drying is the relative stability of the invasion front which can be roughly assimilated to the TC region. As discussed in Masmoudi *et al.* (1992), this stability is observed in the experiments with the micromodel when the gravity forces are not negligible.

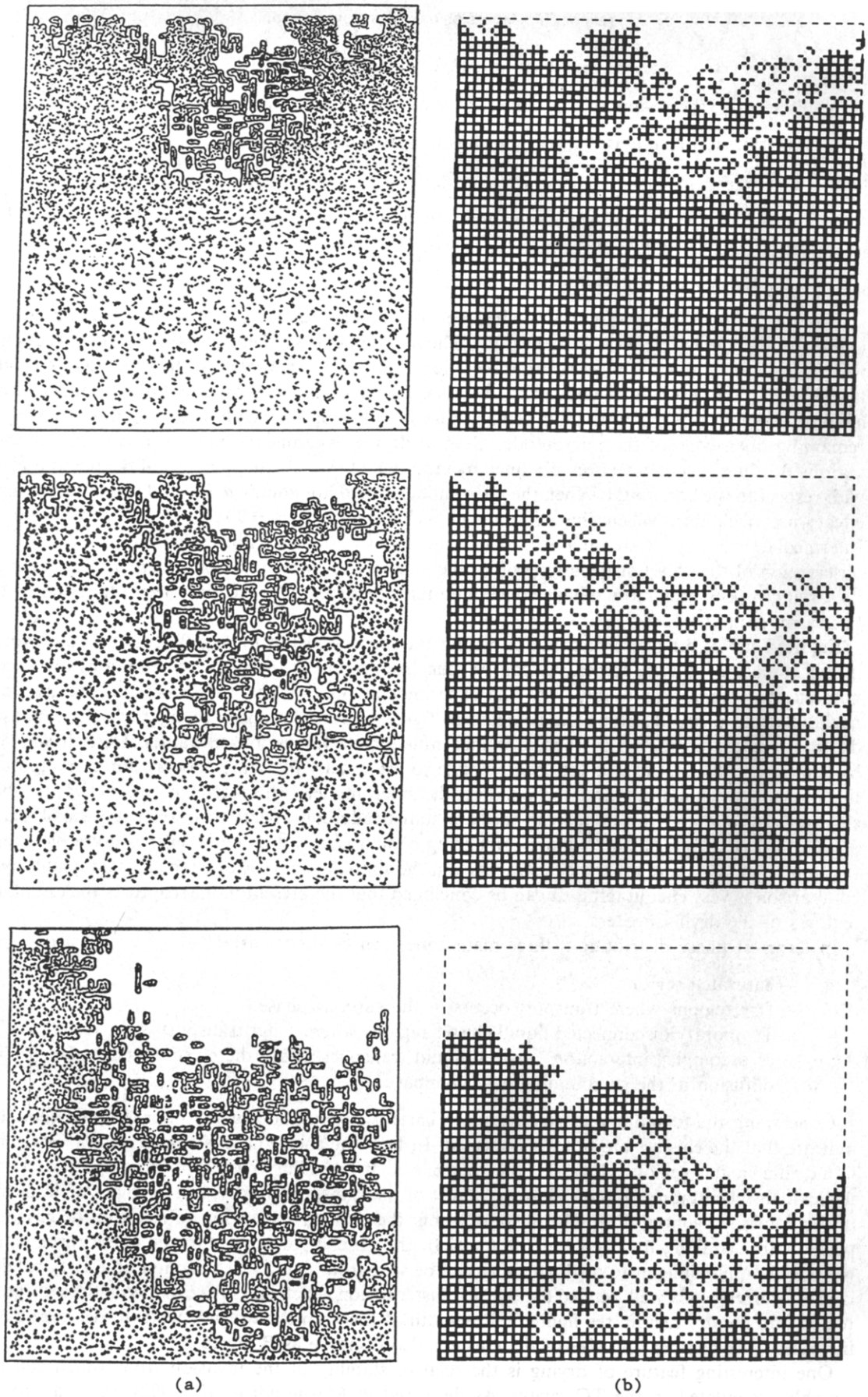

Figure 4. Phase distributions obtained experimentally (a) and numerically (b) in the absence of gravity forces at various stages of drying. Liquid phase in black. Water vapor escapes at the top.

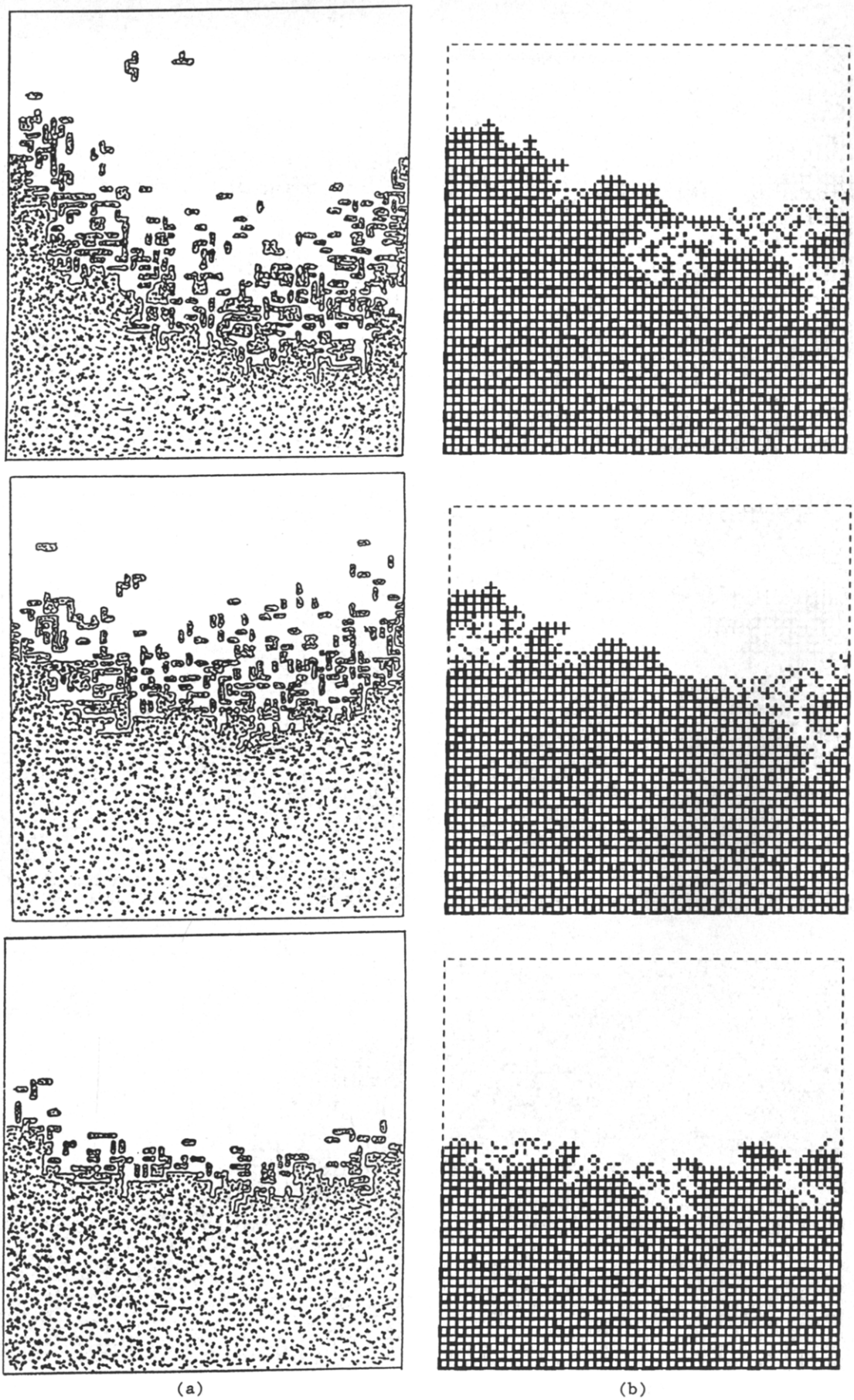

Figure 5. Phase distributions obtained experimentally (a) and numerically (b) for various B values at comparable saturations during drying. Liquid phase in black. Water vapor escapes at the top. B increases from top to bottom.

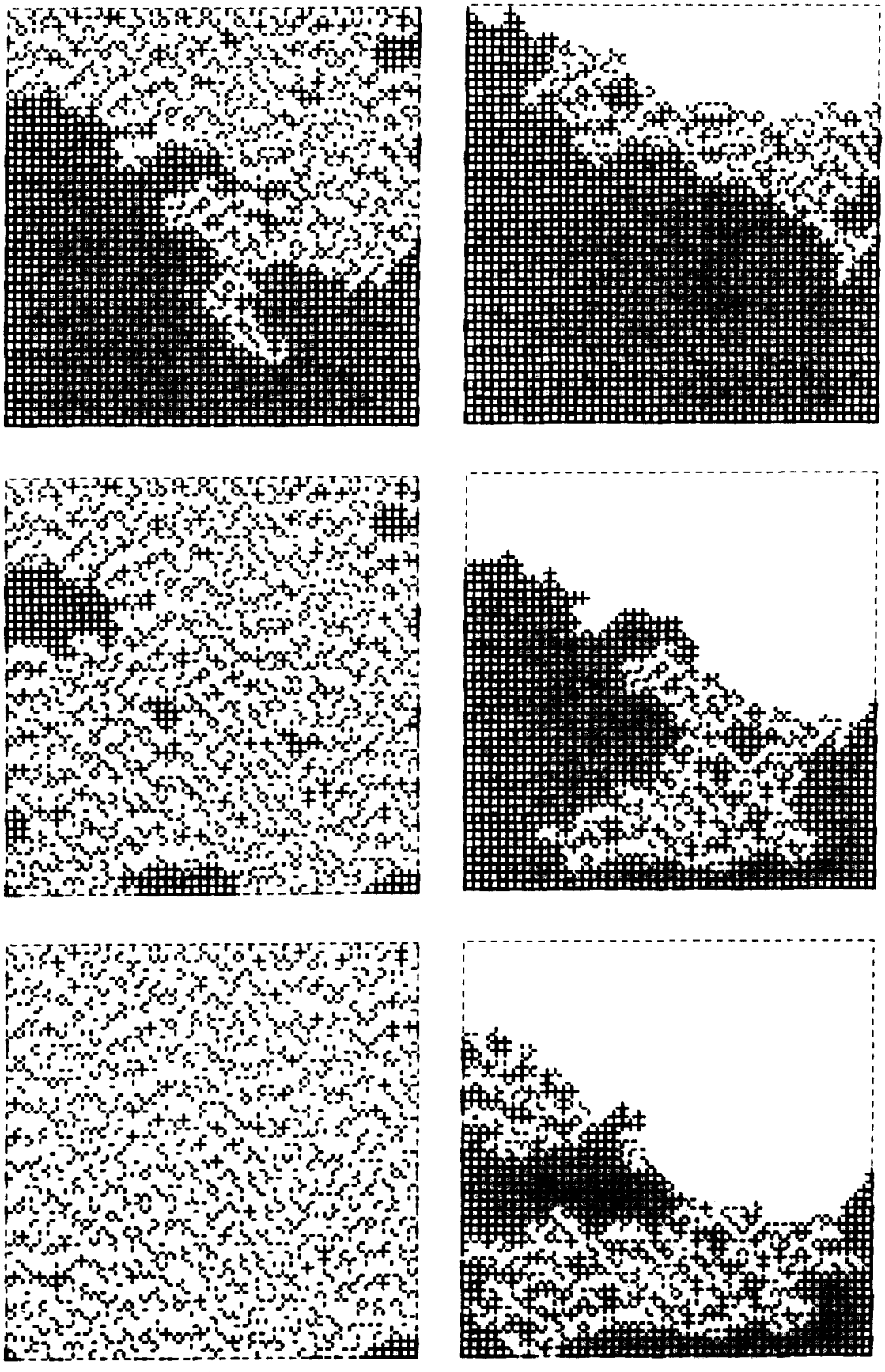

(a) (b)

Figure 6. Phase distributions obtained by using the invasion percolation rules without trapping (a) and by means of the present model (b).

Such a stability is also obtained in the simulations. As a matter of fact, this is not at variance with conventional immiscible displacement at low Ca in the presence of buoyancy forces (Wilkinson 1984). More interestingly, Shaw (1987) has observed the front invasion stability even when gravity seems to be unimportant, as opposed to conventional immiscible displacement at comparable viscosity ratio and Ca which produces unstable fronts that finger. Even though viscous effects were not negligible in Shaw's experiments, we believe that such a front stability would be observed, in the absence of gravity forces, by using the present model if a sufficiently large network was used. Such a front stability could be explained in terms of the removal mechanism of the clusters through the action of evaporation. In other terms, this stability would be one the consequences of the fact that permanent trapping of the liquid does not occur in drying, every cluster being eventually invaded by the gas phase. It should be emphasized that the front stability problem is important from the point of view of the validity of the continuum or macroscopic approach.

It should be clear from the aforementioned simulations that evaporation takes place at each elementary liquid–gas interface. Therefore, the evaporating surface is here quite complicated. In fact, this surface is the gas–liquid interfacial surface.

4.2. Standard invasion percolation without the trapping rule

As trapping does not occur in drying, it could sound attractive to model drying as standard invasion percolation without the trapping rule. Clearly, such a model is simpler and would consume less computer time than the one presented in section 2.2. In the absence of gravity, standard invasion percolation without the trapping rule leads to the phase distributions depicted in figure 6 where the results obtained with our drying model at comparable numbers of invaded throats are also shown. As shown in figure 6, drying cannot be modeled as standard invasion percolation without trapping. Because of the combined actions of evaporation, gas diffusion and capillary mechanisms, the invasion rules given in section 2.2 must be used.

5. CONCLUSIONS

The purpose of this paper has been to present a model of drying in porous media based on a network approach. Contrary to traditional models based on the continuum approach to porous media, the present model enables us to simulate the drying process at the pore level. The model accounts for drying at very low Ca and relies on a modified form of invasion percolation. Contrary to conventional immiscible displacements at low Ca, drying results in no permanent trapping of the wetting fluid. However, drying cannot be modeled as standard invasion percolation without trapping, as has been shown in section 4. The rules describing the invasion process take into account not only the capillary mechanisms but also the evaporation at the non-wetting fluid–wetting fluid interfaces and the diffusion of the vapor in the gaseous phase. Gravity effects are also taken into account in the present model. As the experiments and the simulations show, one important effect of gravity is to limit the width of the invasion front which is the region containing the temporary trapped clusters (TC). Also, gravity results in reducing the size and the number of the TC. On the basis of comparisons with experimental results obtained by means of a micromodel, one can conclude that the model captures the essential features of drying.

It appears that such a microscopic approach allows one to address fundamental questions related to the drying of capillary porous media. These questions include the determination of the macroscopic transport properties associated with a given porous structure and the analysis of convective mass transfer at the interface (Prat 1991). An even more fundamental question is whether the drying can be really described by means of the standard continuum approach. Invoking the present model together with proper averaging techniques seems to be a promising approach for attacking the problem. To exemplify, it is possible to check whether the REV concept is relevant here. Also, it should be emphasized that most of the interfacial convective mass transfer problems and most of the internal macroscopic transport property problems seem to depend on a proper analysis of the transfer occurring in the temporary cluster region. As the simulations

presented in this paper clearly show, it is unjustified to envision transport in this region as the *ad hoc* superposition of vapor diffusion and a generalized Darcy's law type transport in the liquid phase. In reality, transport results from the combined action of vapor diffusion in the gaseous phase and of liquid transport within the temporary clusters. The transport occurring in the liquid phase formed by various disconnected clusters seems to have little to do with Darcy's law even though it can be argued that the liquid clusters under consideration are in fact connected by very thin liquid films.

Naturally, the present model cannot account for all drying situations. It is only valid for initially saturated capillary porous media in which hygroscopic effects are negligible. The drying rate should be low enough to satisfy the low Ca constraint together with the isothermal process assumption. However, the present model is amenable to improvements. Future versions of the model will include thermal effects, adsorption phenomena and the Kelvin effect. Also, the model will be extended to three dimensions in order to obtain more realistic predictions.

Acknowledgements—The author is grateful to C. Zarcone for providing the micromodel, to W. Masmoudi for providing some of the experimental data, to O. A. Plumb for suggesting the trapped cluster detection algorithm used in the model and to D. Poulikakos for improving the paper. Financial support from P.I.R.S.E.M.–C.N.R.S. and Institut Français du Pétrole is gratefully acknowledged. Last but not least, special thanks are due to L. Travé-Massuyes for moral support.

REFERENCES

BACHMAT, Y. & BEAR, J. 1986 Macroscopic modelling of transport phenomena in porous media. 1: the continuum approach. *Transp. Porous Media* **1,** 213–240.

CHANDLER, R., KOPLIK, J., LERMAN, K. & WILLENSEN, J. F. 1982 Capillary displacement and percolation in porous media. *J. Fluid Mech.* **119,** 249–267.

DAIAN, J. F. & SALIBA, J. 1991 Determination d'un r, seau al, atoire de pores pour mod, liser la sorption et la migration d'humidit, dans un mortier de ciment. *Int. J. Heat Mass Transfer* **34,** 2081–2096.

LENORMAND, R., TOUBOUL, E. & ZARCONE, C. 1988 Numerical models and experiments on immiscible displacements in porous media. *J. Fluid Mech.* **189,** 165–187.

MASMOUDI, W. 1990 Contribution à l'étude fondamentale du séchage des matériaux capillaro-poreux. Critique de la modélisation macroscopique et du protocole expérimentale de validation. Thèse I.N.P.Toulouse, France.

MASMOUDI, W., PRAT, M. & BORIES, S. 1992. Drying: percolation theory or continuum approach. Some experimental evidences. In *Heat and Mass Transfer in Porous Media* (Edited by QUINTARD, M. & TODOROVIC, M.), pp. 817–828. Elsevier, New York.

PLUMB, O. A. & PRAT, M. 1992. Microscopic models for the study of drying of capillary porous media. In *Drying '92* (Edited by MUJUMDAR, A. S.), pp. 397–406. Elsevier, New York.

PRAT, M. 1991 2*D* modelling of drying of porous media: influence of edge effects at the interface. *Drying Technol.* **9,** 1181–1208.

QUENARD, D. 1989 Adsorption et transfert d'humidité dans les matériaux hygroscopiques. Thèse I.N.P.Toulouse, France.

SHAW, T. M. 1987 Drying as an immiscible displacement process with fluid counterflow. *Phys. Rev. Lett.* **59,** 1671–1674.

STAUFFER, D. 1985 *Introduction to Percolation Theory*. Taylor & Francis, London.

WHITAKER, S. 1977 Simultaneous heat, mass and momentum transfer in porous media. A theory of drying. In *Advances in Heat Transfer*, Vol. 13. Academic Press, New York.

WILKINSON, D. 1984 Percolation model of immiscible displacement in the presence of buoyancy forces. *Phys. Rev.* **A30,** 520–531.

WILKINSON, D. 1986 Percolation effects in immiscible displacement. *Phys. Rev.* **A34,** 1380–1391.

WILKINSON, D. & WILLEMSEN, J. F. 1983 Invasion percolation: a new form of percolation theory. *J. Phys. A: Math. Gen.* **16,** 3365–3376.

APPENDIX

Vapor Diffusion Computation

Making use of the model requires the solving at each step of the water vapor diffusion equation within the throats and pores occupied by the gaseous phase. For simplicity, several assumptions are made:

- We consider the diffusion process as quasi-steady. Thus, for a given phase distribution within the network, we solve the steady version of the diffusion equation. As the phase distribution changes at each step, the vapor partial pressure field within the gaseous phase is updated at each step.
- A boundary condition should be specified at each elementary liquid–gas interface, figure A1. Assuming that the pores and throats are large enough to neglect the Kelvin effect, the saturation vapor pressure at the selected reference temperature, typically 20°C, is imposed. Therefore, the curvature radius of each elementary interface is supposed to be large enough to not significantly influence the equilibrium vapor pressure at the interface.
- Water films, if any, along the walls of the pores or throats occupied by the gaseous phase are not taken into account.
- One-dimensional transfer is assumed in each throat.
- The vapor partial pressure ϕ is much smaller than the gaseous phase pressure P, i.e.

$$\frac{P}{P-\phi} \approx 1.$$

Under these circumstances, the vapor partial pressure at each "gaseous" node of the network is obtained by expressing the mass flux balance at each node. To exemplify, for the node depicted in figure A1, the mass flux balance is written as

$$F_n + F_s + F_e + F_w = 0, \qquad [A1]$$

in which each elementary mass flux is computed according to table A1. In table A1 ρ, D, e, l, ϕ and ϕ_{sat} are, respectively, the gaseous phase density, the vapor diffusion coefficient, the thickness of the network, the throat width, the vapor partial pressure and the saturation vapor partial pressure. The symbols M_v, R and T stand for the water molecular weight, the gas constant and the reference temperature.

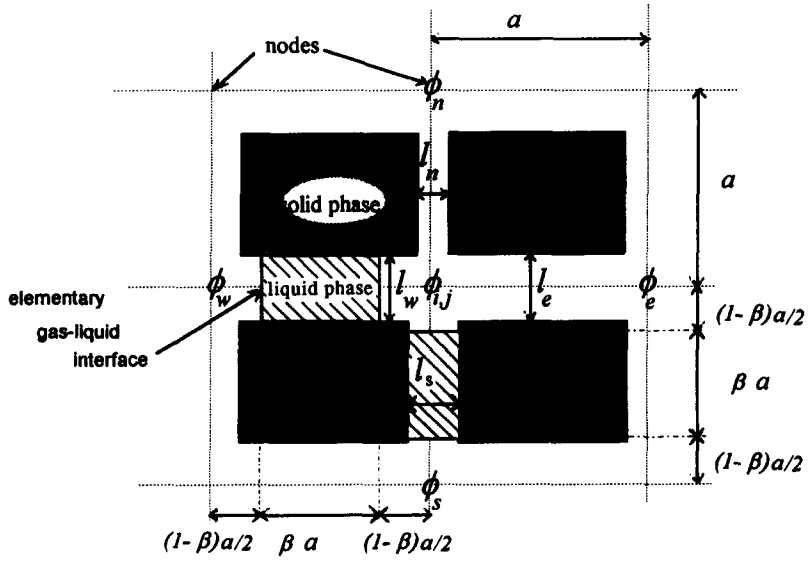

Figure A1. Vapor diffusion computation.

Table A1. Mass flux for the node depicted in figure A1

F_n	$\rho D l_n e \dfrac{M_v}{RT} \dfrac{\phi_n - \phi_{ij}}{a}$
F_s	$\rho D l_s e \dfrac{M_v}{RT} \dfrac{\phi_{sat} - \phi_{ij}}{(1-\beta)(a/2)}$
F_w	$\rho D l_w e \dfrac{M_v}{RT} \dfrac{\phi_{sat} - \phi_{ij}}{(1-\beta)(a/2)}$
F_e	$\rho D l_e e \dfrac{M_v}{RT} \dfrac{\phi_e - \phi_{ij}}{a}$

For a node located at the boundary of the network, the boundary condition is expressed in terms of an external flux through the use of a local mass transfer coefficient. By writing such a mass flux balance for each "gaseous" node of the system, we end up with a linear system of as many equations as gaseous nodes. This linear system is solved utilizing a standard routine. With the above information, the mass flux at the boundary of each TC can be computed.